

Electrochemical and quantum chemical studies on phthalhydrazide as corrosion inhibitor for mild steel in 1 M HCl solution

Ahmed Y. Musa · Abu Bakar Mohamad ·
Mohd Sobri Takriff · Ramzi T. T. Jalgham

Received: 24 July 2011 / Accepted: 9 August 2011
© Springer Science+Business Media B.V. 2011

Abstract The inhibition ability of phthalhydrazide (PTD) for mild steel in 1 M HCl at 30 °C was investigated by electrochemical measurements [impedance spectroscopy (EIS) and potentiodynamic polarization techniques] and quantum chemical calculations. The frontier molecular orbital energy E_{HOMO} (highest occupied molecular orbital), E_{LUMO} (lowest unoccupied molecular orbital), and the Mulliken charge distribution were calculated and are discussed. Results showed that the inhibition efficiency of PTD increased with inhibitor concentration. The maximum corrosion inhibition efficiency was 77.6% at 2 mM PTD. Adsorption of the inhibitor followed the Langmuir adsorption isotherm. Adsorption of inhibitor molecules on mild steel surface occurred spontaneously and chemically. Quantum chemical calculations showed that the low performance of PTD as a corrosion inhibitor is due to the large energy gap ($E_{\text{HOMO}} - E_{\text{LUMO}}$).

Keywords Acid corrosion · Corrosion inhibitor · EIS · Quantum chemical calculations

Introduction

Hydrochloric acid solution is used in pickling, industrial acid cleaning, acid descaling, and oil-well acidizing. Due to the aggressive nature of HCl, the practice of inhibition is commonly used to reduce corrosive attack of metallic materials. Inhibitors are generally used in this process to control metal dissolution as well as acid consumption [1]. Heterocyclic compounds containing sulfur, nitrogen, and oxygen have been used as very effective inhibitors against corrosion of mild steel in

A. Y. Musa (✉) · A. B. Mohamad · M. S. Takriff · R. T. T. Jalgham
Department of Chemical and Process Engineering, Universiti Kebangsaan Malaysia, 43600 Bangi, Selangor, Malaysia
e-mail: ahmed.musa@ymail.com; ahmedym@eng.ukm.my

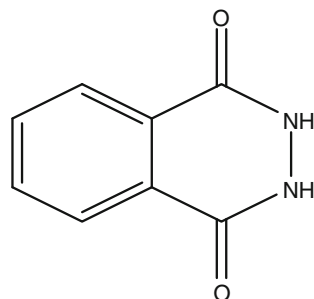
acidic media [1–3]. Existing data show that most organic inhibitors act by adsorption on the metal surface. Adsorption of inhibitors is influenced by the nature and surface charge of the metal, the type of electrolyte used, and the chemical structure of the inhibitor [4]. Theoretical chemistry has been used recently to explain the mechanism of corrosion inhibition, e.g., through quantum chemical calculations [5]. Quantum chemical calculations have proved to be a very powerful tool for studying this mechanism [6].

The aim of this study is to investigate the effect of addition of PTD (Fig. 1) on corrosion resistance for mild steel in 1 M HCl solution at 30 °C. Electrochemical impedance spectroscopy (EIS) and potentiodynamic polarization techniques were utilized in this study. Theoretical studies on electronic and molecular structures of PTD were conducted using quantum chemical calculations performed based on parameterized model 3 (PM3), Austin model 1 (AM1), and modified neglect of differential overlap (MNDO) semi-empirical equations at restricted Hartree–Fock (RHF) level.

Materials and experiments

The studied compound PTD was purchased from Sigma-Aldrich Co. and was tested without any further purification. PTD was used in the concentration range 0.25–2 mM. Mild steel specimens obtained from the Metal Samples Company were used as the working electrodes throughout the study. The composition (wt. %) of the mild steel was: Fe, 99.21; C, 0.21; Si, 0.38; P, 0.09; S, 0.05; Mn, 0.05; Al, 0.01, with exposed area of 4.5 cm². The specimens were cleaned according to ASTM standard G1-03 [7]. Electrochemical measurements were conducted using a Gamry water-jacketed glass cell. The cell contained three electrodes, i.e., the working, counter, and reference electrodes, consisting of mild steel, a graphite bar, and a saturated calomel electrode (SCE), respectively. Measurements were performed using a Gamry Instrument potentiostat/galvanostat/ZRA Ref 600 model. EIS measurements were performed at corrosion potentials (E_{corr}) over a frequency range of 10 kHz to 0.1 Hz with signal amplitude perturbation of 10 mV. Potentiodynamic current–potential curves were recorded by changing the electrode potential automatically from –0.2 to 0.2 V at scan rate of 0.5 mV s^{–1}. The numerical values of corrosion current density (j_{corr}), corrosion potential (E_{corr}), anodic Tafel slope (β_{A}), and cathodic Tafel slope (β_{C}) were calculated from the Tafel fit routine provided by Gamry Echem Analyst

Fig. 1 Chemical structure of phthalhydrazide (PTD)



software, which uses nonlinear chi-squared minimization to fit the data to the Stern–Geary equation. The fit uses four adjustable parameters: j_{corr} , E_{corr} , β_{A} , and β_{C} . The minimization algorithm makes a number of estimates for the values of the four parameters. After each estimate, the goodness of fit is evaluated. A new estimate for the parameter values is then made, using the well-known Marquardt algorithm. The process is repeated until the fit stops improving. Electrochemical measurements were initiated about 30 min after the working electrode was immersed in solution to reach the steady-state potential.

The quantum chemical parameters were calculated using Material Studio version 5.5, a high-quality quantum mechanics computer program (available from Accelrys, San Diego, CA). These calculations employed PM3, AM1, and MNDO semi-empirical equations at RHF level implemented in the VAMP module. First, the molecule was sketched, then optimized with the VAMP module.

Results and discussion

EIS measurements

EIS measurements were used in this study to investigate the corrosion behavior of mild steel in 1 M HCl solution without and with various concentrations of PTD

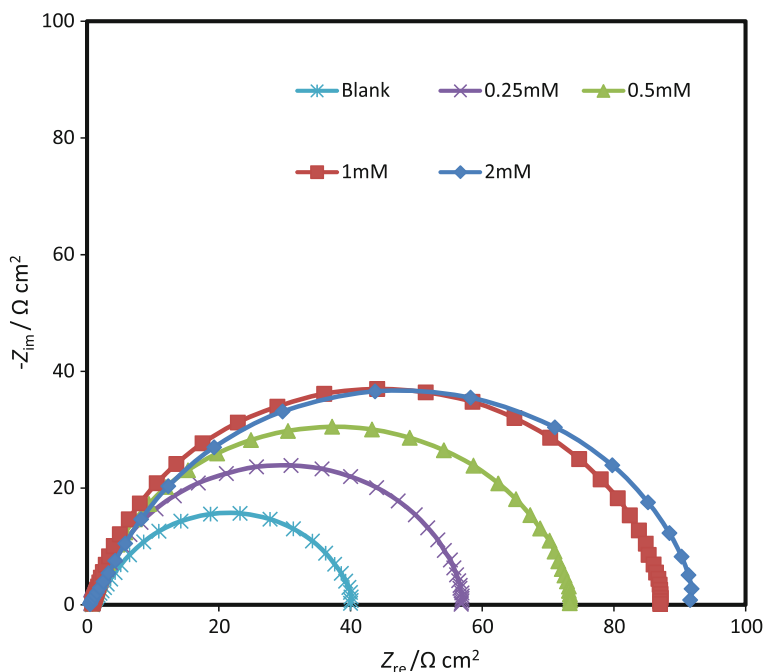


Fig. 2 Nyquist plots for mild steel in 1 M HCl at 30 °C in absence and presence of various concentrations of PTD

at 30 °C. Nyquist plots for mild steel in 1 M HCl at 30 °C are shown Fig. 2. The impedance of inhibited mild steel increased with increasing PTD concentration. A depressed semicircle could be attributed to different physical phenomena such as roughness and inhomogeneities of the solid surfaces, impurities, grain boundaries, and distribution of surface-active sites, therefore the capacitance is represented as a constant-phase element (CPE). A CPE is defined in the impedance representation as follows [8, 9]:

$$Z(\omega) = Z_0(Y\omega)^{-\alpha}, \quad (1)$$

where Z_0 is the CPE constant, ω is the angular frequency (in rad/s), $Y^2 = -1$ defines imaginary numbers, and α is the CPE exponent.

The electrochemical systems can be represented using the simplified CPE equivalent circuit shown in Fig. 3, which shows a parallel combination of the charge-transfer resistance (R_{ct}) and constant-phase element related to the capacity of the double layer (CPE_{dl}), both in series with the solution resistance (R_s). The inhibition efficiency was calculated according to Eq. 2.

$$IE\% = \left(1 - \frac{R_{ct}^0}{R_{ct}}\right) \times 100, \quad (2)$$

where R_{ct} and R_{ct}^0 are the charge-transfer resistance with and without PTD, respectively. The fitted circuit values R_{ct} and IE% are listed in Table 1. It can be seen that the CPE tends to decrease while R_{ct} and the inhibition efficiency increase with increasing PTD concentration. This suggests that inhibitor molecules are absorbed on the mild steel surface, to protect its surface from corrosion.

Fig. 3 Equivalent circuit modal used to fit the experimental data for mild steel in 1 M HCl in absence and presence of various concentrations of PTD

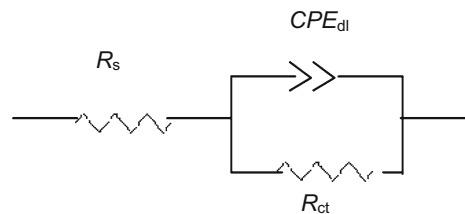


Table 1 Fitted impedance parameters for mild steel in 1 M HCl solution in absence and presence of different concentrations of PTD at 30 °C

| C_{inh}/mM | $R_s/\Omega \text{ cm}^2$ | $R_{ct}/\Omega \text{ cm}^2$ | $CPE_0, \mu(S \times s^z/cm^2)$ | α | IE% |
|--------------|---------------------------|------------------------------|---------------------------------|----------|------|
| 0 | 1.07 | 42 | 774 | 0.78 | 0.00 |
| 0.25 | 0.85 | 87.4 | 299 | 0.83 | 51.9 |
| 0.5 | 1.09 | 111.3 | 229.2 | 0.85 | 62.3 |
| 1 | 1.21 | 131.8 | 176.3 | 0.87 | 68.1 |
| 2 | 0.62 | 143.7 | 322 | 0.78 | 70.8 |

Potentiodynamic polarization

Potentiodynamic polarization curves for mild steel in 1 M HCl solution at 30 °C without and with various concentration of PTD are presented in Fig. 4. The values of corrosion current density (j_{corr}), corrosion potential (E_{corr}), anodic Tafel slope (β_{A}), and cathodic Tafel slope (β_{c}) are listed in Table 2. It can be seen from Table 2 that the j_{corr} values decreased with increasing PTD concentration. A compound can be classified as an anodic- or a cathodic-type inhibitor when the change in the E_{corr} value is larger than 85 mV [5]. Since the largest displacement exhibited by PTD is 12 mV (Table 1), PTD is considered as a mixed-type inhibitor. Nevertheless, Fig. 4 shows that the decreases in the anodic part are more pronounced than in the cathodic part, meaning that addition of PTD to 1.0 M HCl solution will reduce anodic

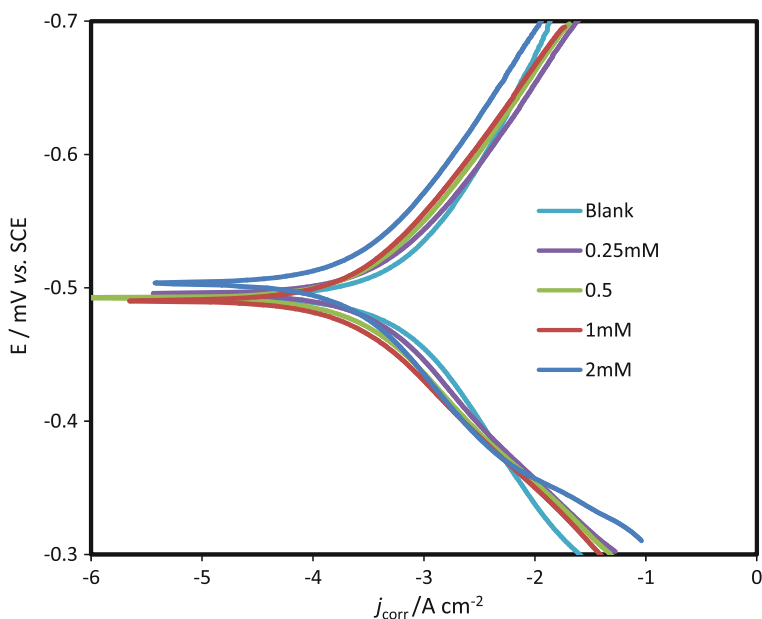


Fig. 4 Potentiodynamic polarization curves for mild steel in 1 M HCl at 30 °C in absence and presence of various concentrations of PTD

Table 2 Polarization parameters of mild steel in 1 M HCl solution in absence and presence of different concentration of PTD at 30 °C

| C_{inh}/mM | $\beta_{\text{A}}/\text{V decade}^{-1}$ | $\beta_{\text{c}}/\text{V decade}^{-1}$ | $j_{\text{corr}}/\mu\text{A cm}^{-2}$ | $E_{\text{corr}}/\text{mV versus SCE}$ | IE% |
|----------------------------|-----------------------------------------|-----------------------------------------|---------------------------------------|----------------------------------------|------|
| 0 | 0.12 | 0.14 | 660 | −491 | 0 |
| 0.25 | 0.097 | 0.109 | 245 | −496 | 62.9 |
| 0.5 | 0.089 | 0.107 | 182 | −492 | 72.4 |
| 1 | 0.086 | 0.106 | 155 | −490 | 76.5 |
| 2 | 0.093 | 0.111 | 148 | −503 | 77.6 |

dissolution of mild steel more than the cathodic hydrogen evolution reaction. The IE% values listed in Table 2 were calculated according to Eq. 3.

$$\text{IE\%} = \left(1 - \frac{j_{\text{corr(inh)}}}{j_{\text{corr(uninh)}}} \right) \times 100, \quad (3)$$

where $j_{\text{corr(uninh)}}$ and $j_{\text{corr(inh)}}$ are the corrosion current densities in the absence and presence of inhibitor, respectively. The IE% values increased as the inhibitor concentration increased; this result follows the same trend as IE% obtained from the EIS measurements.

Adsorption isotherm model

Adsorption isotherm calculations of the PTD on the mild steel surface were performed to investigate the mechanism of corrosion inhibition. It was assumed that the adsorption of this inhibitor followed the Langmuir adsorption isotherm. The Langmuir adsorption isotherm, which is presented by Eq. 4, is most often used to calculate the equilibrium constant (K_{ads}).

$$\frac{C_{\text{inh}}}{\theta} = \frac{1}{K_{\text{ads}}} + C_{\text{inh}}. \quad (4)$$

The values of θ in Eq. 4, representing the degree of surface coverage, were obtained from potentiodynamic data and calculated as follows:

$$\theta = \frac{\text{IE\%}}{100}. \quad (5)$$

Figure 5 shows that a plot of C_{inh}/θ versus C_{inh} yields a straight line with $R^2 = 0.9998$ and intercept of 0.1693. The adsorption free energy was calculated using Eq. 6.

$$\Delta G_{\text{ads}} = -RT \ln(55.5 K_{\text{ads}}). \quad (6)$$

The calculated value of ΔG_{ads} was $-34.16 \text{ kJ mol}^{-1}$. The calculated value of ΔG_{ads} was found to be negative with value around -40 kJ mol^{-1} , indicating that the adsorption mechanism of inhibitor on mild steel surface occurred spontaneously and chemically [8].

Quantum chemical calculations

The calculated quantum chemical parameters by PM3, AM1, and MNDO semi-empirical equations are listed in Table 3. The distributions of the orbital energy for the PTD molecule based on the PM3 semi-empirical equation are shown in Fig. 6. Some quantum chemical parameters are related to the interactions between the inhibitor and the metal surface. E_{HOMO} is often associated with the capacity of a molecule to donate electrons. An increase in the value of E_{HOMO} can facilitate adsorption and thereby the inhibition efficiency, indicating disposition of the molecule to donate orbital electrons to an appropriate acceptor with empty

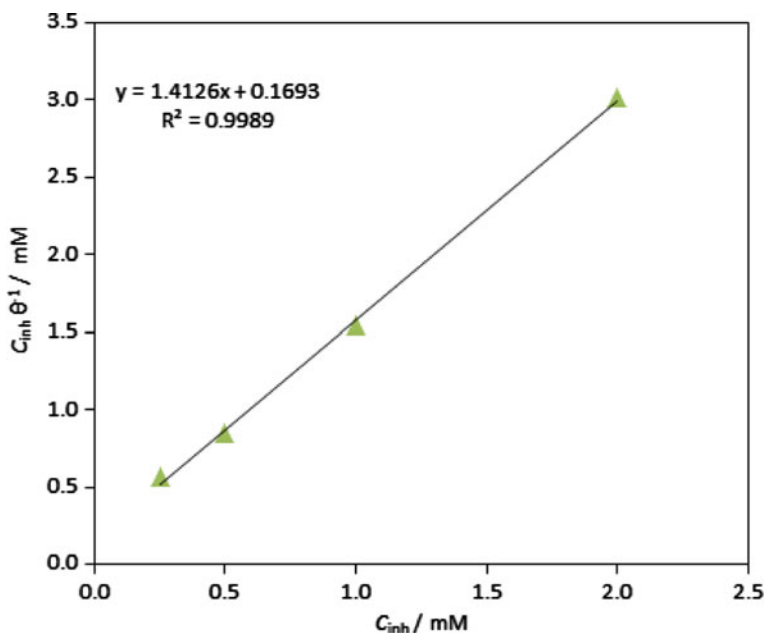


Fig. 5 Adsorption isotherm of PTD molecules on mild steel surface in 1 M HCl at 30 °C

Table 3 Quantum parameters for PTD calculated with PM3, AM1, and MNDO semi-empirical equations

| | E_{HOMO}/eV | E_{LUMO}/eV | $E_{HOMO} - E_{LUMO}/\text{eV}$ |
|------|----------------------|----------------------|---------------------------------|
| PM3 | -9.685 | -1.112 | -8.573 |
| AM1 | -9.785 | -1.013 | -8.772 |
| MNDO | -10.012 | -1.124 | -8.887 |

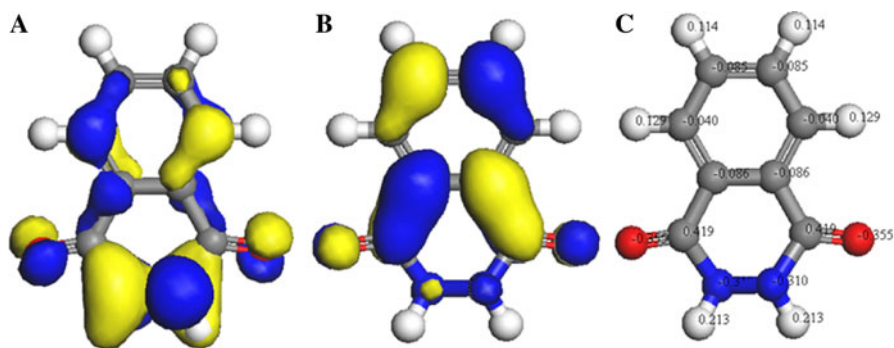


Fig. 6 **a** E_{HOMO} , **b** E_{LUMO} , and **c** Mulliken atomic charge distribution of PTD molecule calculated by PM3 semi-empirical equation

molecular orbitals [5]. Therefore, E_{LUMO} indicates the ability of the molecule to accept electrons. The lower the value of E_{LUMO} , the more probable it is that the molecule will accept electrons. Consequently, low absolute values of the energy band gap ($E_{\text{HOMO}} - E_{\text{LUMO}}$) will render good inhibition efficiencies, because the energy to remove an electron from the highest occupied orbital will be low [9, 10]. The calculated quantum chemical parameters (Table 3) reveal that PTD has high HOMO and low LUMO, with a large energy gap. This large energy gap corresponds to the low inhibitory performance of the PTD. The Mulliken atomic charge distribution calculated using the PM3 semi-empirical equation is presented in Fig. 6. It can be readily observed that oxygen, nitrogen, and some carbon atoms have higher charge densities. The regions of highest electron density are generally the sites at which electrophiles will attack. Therefore, O, N, and C atoms were active centers, having the strongest bonding ability to the metal surface. On the other hand, the HOMO (Fig. 6) was mainly distributed on the area containing nitrogen atom. Thus, the area containing nitrogen atom was probably the primary site for bonding.

Based on the above discussion, it could be deduced that PTD, apart from existing in the cationic form which can interact with the mild steel surface by electrostatic attraction, may also interact with the mild steel surface using a number of active centers, forming a good protective layer on the mild steel surface and thus retarding further corrosion of the metal in hydrochloric acid solution.

Conclusions

PTD shows low inhibition efficiency for mild steel in 1 M HCl solution, ranging between 51.9% and 77.6% at 0.25 and 2 mM, respectively. R_{ct} and j_{corr} values were found to increase and decrease with addition of PTD, respectively. Potentiodynamic measurements revealed that PTD acts as a mixed-type inhibitor but with a more pronounced anodic part. Based on thermodynamic parameters, adsorption of this inhibitor on mild steel surface occurred spontaneously and chemically. The large energy gap ($E_{\text{HOMO}} - E_{\text{LUMO}}$) contributed to the low inhibitory performance of PTD.

Acknowledgments We gratefully acknowledge National University of Malaysia (no. UKM-GGM-NBT-037-2011) for support of this work.

References

1. F. Bentiss, C. Jama, B. Mernari, H. El Attari, L. El Kadi, M. Lebrini, M. Traisnel, M. Lagrenée, *Corros. Sci.* **51**, 1628 (2009)
2. Q. Zhang, Y. Hua, *Acta Phys. Chim. Sin.* **27**, 655 (2011)
3. L.J. Berchmans, V. Sivan, S. Venkata, K. Iyer, *Mater. Chem. Phys.* **98**, 395 (2006)
4. F. Bentiss, M. Traisnel, H. Vezin, M. Lagrenée, *Ind. Eng. Chem. Res.* **39**, 3732 (2000)
5. A.Y. Musa, A.A.H. Kadhum, A.B. Mohamad, A.A.B. Rahoma, H. Mesmari, *J. Mol. Struct.* **969**, 233 (2010)

6. M.G.V. Satyanarayana, V. Himabindu, Y. Kalpana, M.R. Kumar, K. Kumar, J. Mol. Struct. **912**, 113 (2009)
7. ASTM G1-3, Standard practice for preparing, cleaning, and evaluating corrosion test specimens
8. A.Y. Musa, A.A.H. Kadhum, A.B. Mohamad, M.S. Takriff, A.R. Daud, S.K. Kamarudin, N. Muhamad, Corros. Eng. Sci. Tech. **45**, 163 (2010)
9. A.Y. Musa, A.A.H. Kadhum, A.B. Mohamad, M.S. Takriff, A.R. Daud, S.K. Kamarudin, Corros. Sci. **52**, 526 (2010)
10. I. Lukovits, K. Pálfi, I. Bakò, E. Kálmán, Corrosion **53**, 915 (1997)